

Supporting Information

Electrocatalytic Water Oxidation Performance in an Extended Porous Organic Framework with a Covalent Alliance of Distinct Ru-Sites

Bishal Boro,^{a,b} Mrinal K. Adak,^c Sohag Biswas,^d Chitra Sarkar,^{a,b} Yogendra Nailwal,^e Abhijit Shrotri,^f Biswarup Chakraborty*,^c Bryan M. Wong*,^d & John Mondal*,^{a,b}

^aDepartment of Catalysis & Fine Chemicals, CSIR-Indian Institute of Chemical Technology, Uppal Road, Hyderabad-500007, India, Email: johnmondal@iict.res.in; johncuchem@gmail.com

^bAcademy of Scientific and Innovative Research (AcSIR), Ghaziabad- 201002, India.

^cDepartment of Chemistry, Indian Institute of Technology Delhi, Hauz Khas, 110016, New Delhi, India. Email: cbiswarup@chemistry.iitd.ac.in

^dDepartment of Chemical & Environmental Engineering, Materials Science & Engineering Program, Department of Chemistry, and Department of Physics & Astronomy, University of California-Riverside, Riverside, California 92521, United States. Email: bryan.wong@ucr.edu

^eDepartment of Chemical Sciences, Indian Institute of Science Education and Research (IISER) Mohali, Sector 81, Knowledge City, Manauli 140306, India.

^fInstitute for Catalysis, Hokkaido University, Kita 21 Nishi 10, Kita-ku, Sapporo, Hokkaido 001-0021, Japan.

Table of Contents

Entry	Content	Page No.
1	Materials and methods	S3
2	Characterization techniques	S3-S4
3	^1H NMR spectrum of (Ru(demob)$_3$Cl$_2$)	S5
4	^{13}C NMR spectrum of (Ru(demob)$_3$Cl$_2$)	S6
5	ESI-MS spectrum of (Ru(demob)$_3$Cl$_2$)	S7
6	Thermal gravimetric analysis (TGA) plots of Ru@Bpy-POP	S8
7	Wide-angle powder X-ray diffraction pattern of Ru@Bpy-POP	S9
8	FT-IR spectrum of Ru@Bpy-POP	S10
9	TEM images of Ru@Bpy-POP	S11
10	FE-SEM images of Ru@Bpy-POP	S12
11	XPS survey spectrum of Ru@Bpy-POP	S13
12	Cyclic voltammetry of Ru@Bpy-POP & RuO $_2$	S14
13	TEM images of reused catalyst Ru@Bpy-POP	S15
14	FE-SEM images of reused catalyst Ru@Bpy-POP	S16
15	Polarization curve obtained from the mass normalized activity of Ru@Bpy-POP and RuO $_2$.	S17
15	References	S18

Materials and methods:

Materials

4,4'-Dimethoxy-2,2'-bipyridine and carbazole were purchased from TCI Chemicals (India) Pvt. Ltd. $\text{RuCl}_3 \cdot x\text{H}_2\text{O}$, sodium hypophosphite, and ammonium chloride were purchased from Sigma Aldrich. Ethanol (EtOH), Nitromethane (NM), Tetrahydrofuran (THF), Acetone, and Methanol (MeOH) were purchased from Finer. All the chemicals were used as received without further purification.

Characterization Techniques:

Powder X-ray diffraction (XRD) patterns of the catalysts were performed with a Bruker D8 Advance X-ray diffractometer operated at a voltage of 40 kV and a current of 40 mA by using Ni-filtered $\text{Cu K}\alpha$ ($\lambda = 0.15406$ nm) radiation. Data were recorded in the 2θ range from 10 to 80° in a continuous scanning mode with a 0.01° sampling pitch and 5° min^{-1} scan rate. The morphology of the catalysts was obtained by scanning electron microscopy (SEM). Field-emission scanning electron microscopic images of samples were obtained using a JEOL JEM 6700 field-emission scanning electron microscope (FE-SEM) equipped with an Energy-Dispersive Spectroscopy (EDS) detector. The elemental mapping EDS analysis was also performed on the same SEM instrument. High-resolution transmission electron microscopy (HR-TEM) images were recorded with a JEOL JEM 2010 transmission electron microscope with an operating voltage 200 kV equipped with a FEG. STEM images were obtained in a JEOL JEM-ARM200F atomic resolution electron microscope at an acceleration voltage of 200 kV equipped with an EDS detector EX-24221M1G5T, has a guaranteed resolution of 0.08 nm. Nitrogen sorption isotherms were obtained by using a Quantachrome Autosorb 1C surface area analyzer at 77 K. Prior to the measurements, the samples were degassed at 140°C for approximately 6 h under high-pressure vacuum. Surface areas were calculated from the adsorption data by using the Brunauer-Emmett-Teller (BET) method in the relative pressure (P/P_0) range of 0.01-0.1. The total pore volumes and pore size distribution curves were obtained from the adsorption branches using non-local density functional theory (NLDFT) methods. X-ray photoelectron spectroscopy (XPS) was investigated on a Thermo Scientific K-Alpha instrument (monochromatic $\text{Al K}\alpha$ radiation, $E_{\text{photon}} = 1486.6$ eV). The binding energy (B.E) in each case (i.e., core levels and valence band maxima) were corrected using an

internal reference of C-1 s peak centered at 284.8 eV. An FT-IR spectrum of the catalysts was investigated on a DIGILAB (USA) IR spectrometer using the KBr disc method. Solid-state ^{13}C CP MAS NMR studies were performed using a Bruker Avance III HD400 MHz NMR spectrometer.

Electrochemical measurements of the **Ru@Bpy-POP** were done with a potentiostat (Gamry instrument) instrument, which is controlled by the Gamry Echem Analyst software. During our electrocatalytic measurement, a reference electrode (Hg/HgO), a counter electrode (Pt), and a catalyst doped working electrode (**Ru@Bpy-POP/NF**) were used in a three-electrode setup. In the electrocatalytic study, 1 M aqueous KOH solution was used as an electrolyte. Cyclic voltammetry (CV) and linear sweep voltammetry (LSV) of the catalysts were investigated in the potential range of 0 to 1V for the oxygen evolution reaction (OER) under a 1 mV s⁻¹ scan rate. The potential of the reference electrode was determined according to the following equation. $E(\text{RHE}) = E(\text{Hg/HgO}) + 0.098\text{V} + (0.059 \times \text{pH}) \text{V}$. The Tafel slope was determined from the LSV plot. In the Tafel plot, overpotentials (η) vs. the logarithm of current density were plotted. The Tafel slope was determined from the following equation:

$$\eta = b \log(j) + a$$

where η , j , and b indicate the overpotential value, current density, and Tafel slope respectively. The double-layer capacitance (C_{dl}) value was used to determine the active surface area on the electrode. For C_{dl} values, different CV curves were recorded (-0.05 V to +0.05 V) at 10, 25, 50, 100, 150, and 200 mV s⁻¹ scan rates. The electrochemically active surface area (ECSA) was calculated from the following relation

$$ECSA = \frac{C_{dl}}{C_s}$$

In 1 (M) KOH, the C_s value for NF is 1.7 mF cm⁻².¹

Electrochemical impedance spectroscopy (EIS) of the R-1 electrode was done within the frequency range 100 to 1 MHz solution resistance (R_s), and the charge transfer resistance (R_{ct}) at the working electrode was determined from the Nyquist plot. For the stability test, a chronoamperometry study was done for 12 h with a constant current density of 10 mA cm⁻².

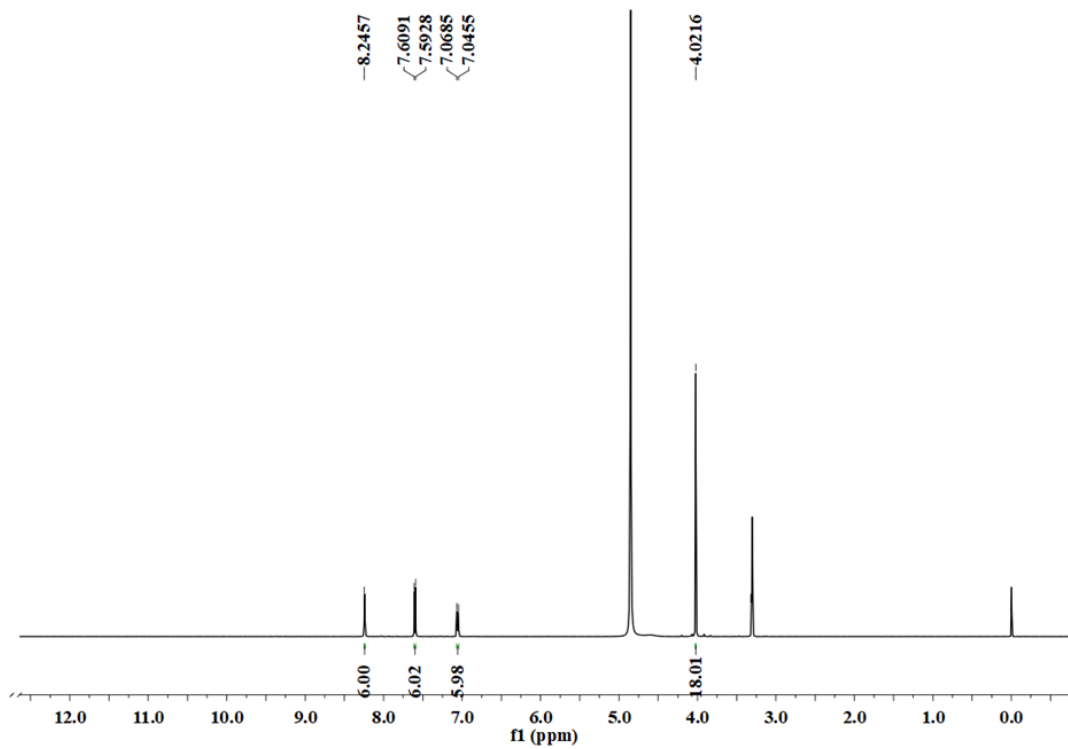


Figure S1: ¹H NMR spectrum of (Ru(demob)₃Cl₂) in CD₃OD solvent.

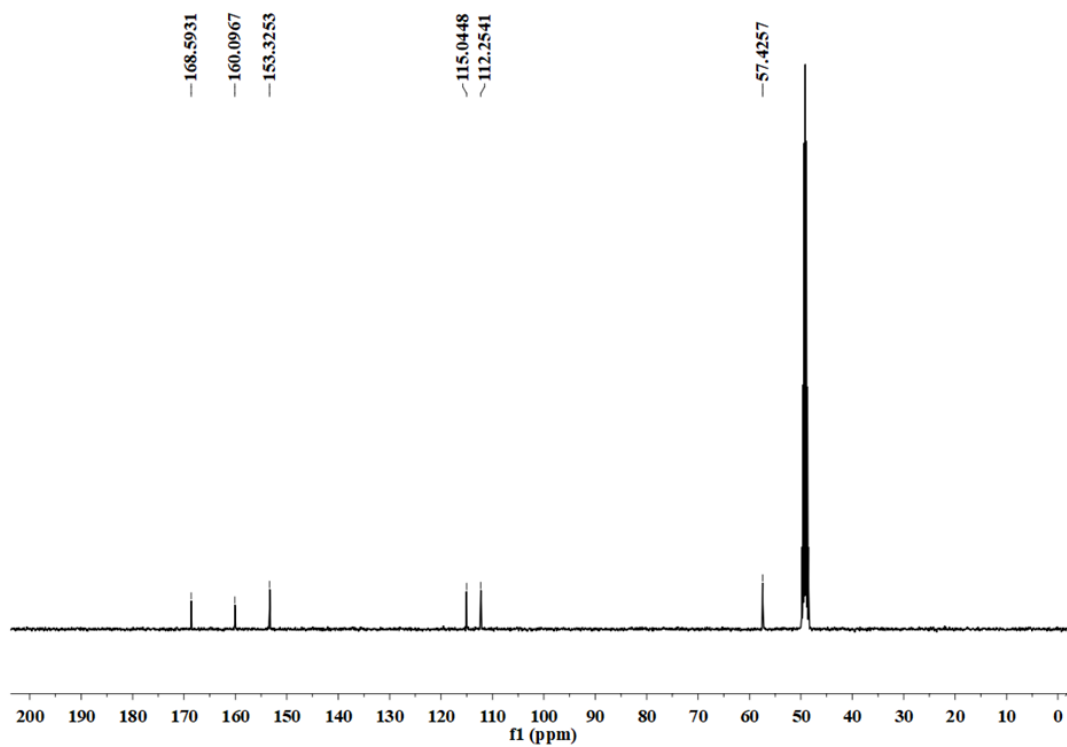


Figure S2: ^{13}C NMR spectrum of $(\text{Ru}(\text{demob})_3\text{Cl}_2)$ in CD_3OD solvent.

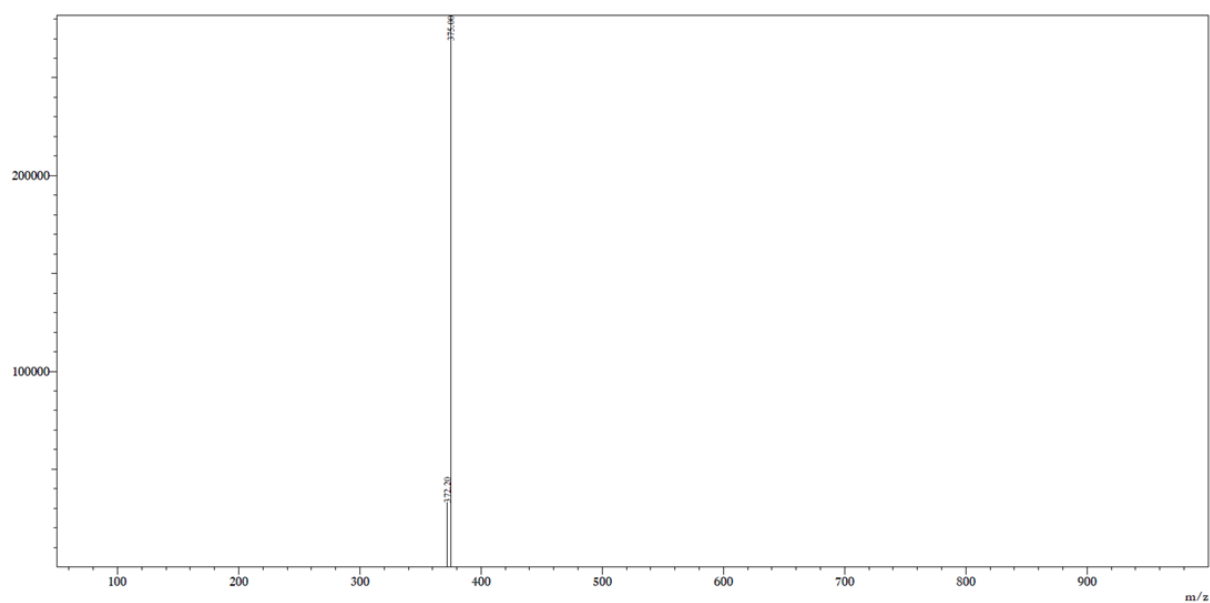


Figure S3: ESI-MS spectrum of $(\text{Ru}(\text{demob})_3\text{Cl}_2)$ in CH_3CN solvent.

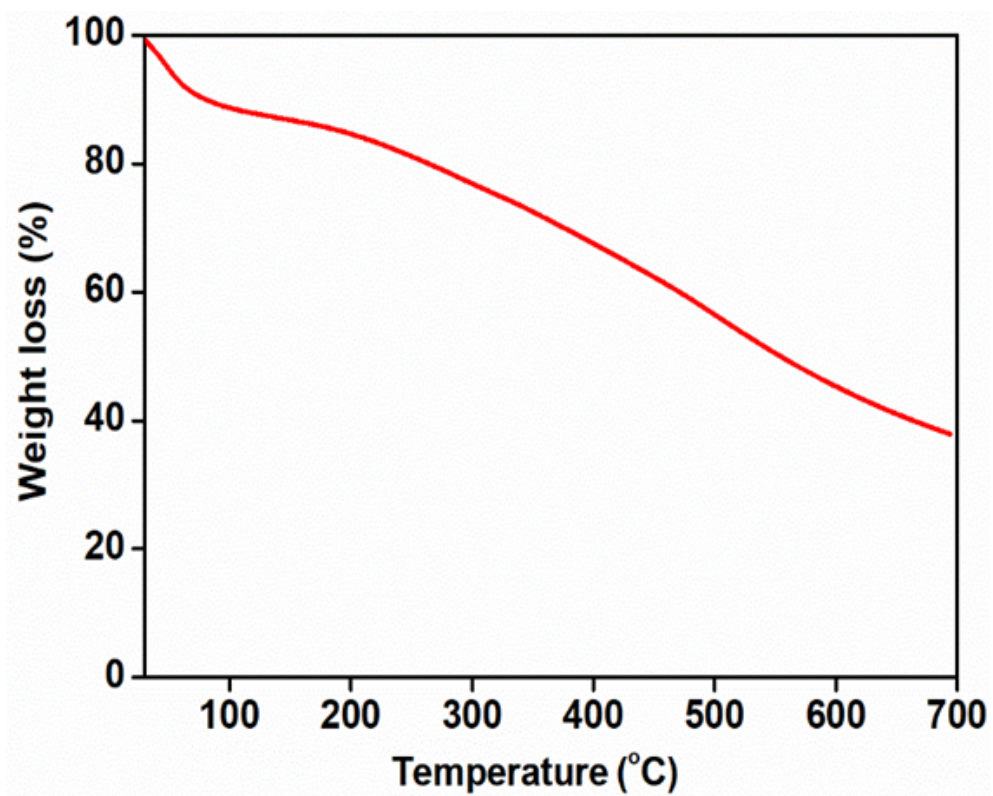


Figure S4: Thermo gravimetric analysis (TGA) plot of Ru@Bpy-POP.

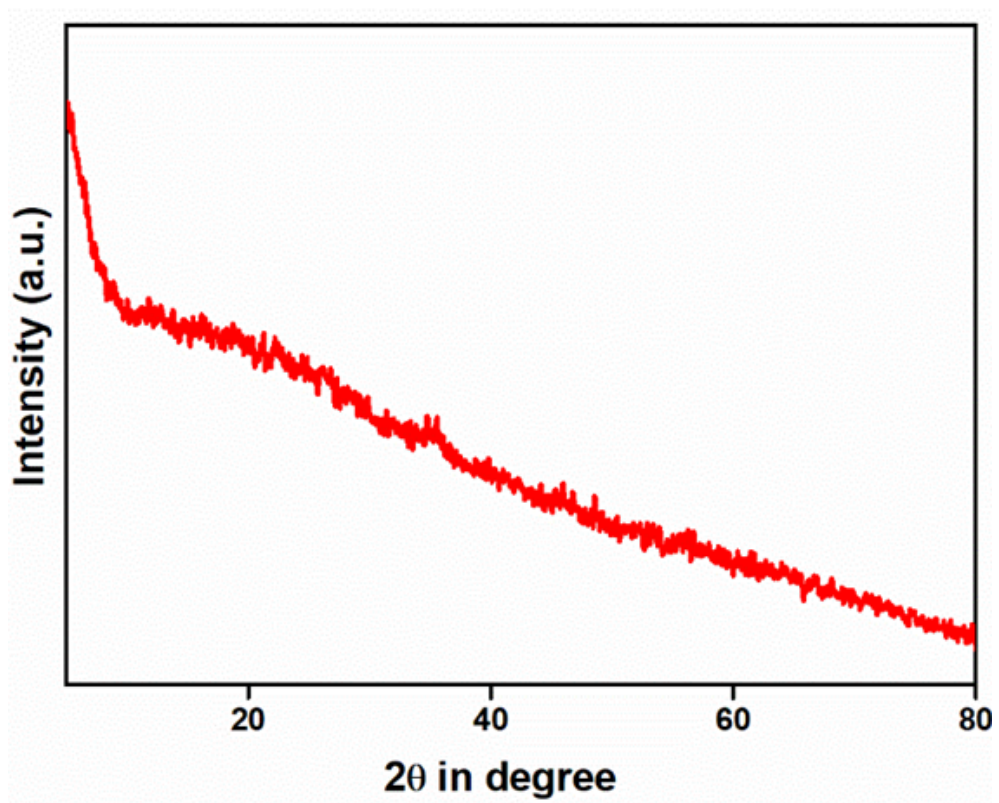


Figure S5: Wide angle powder X-ray diffraction pattern of **Ru@Bpy-POP**.

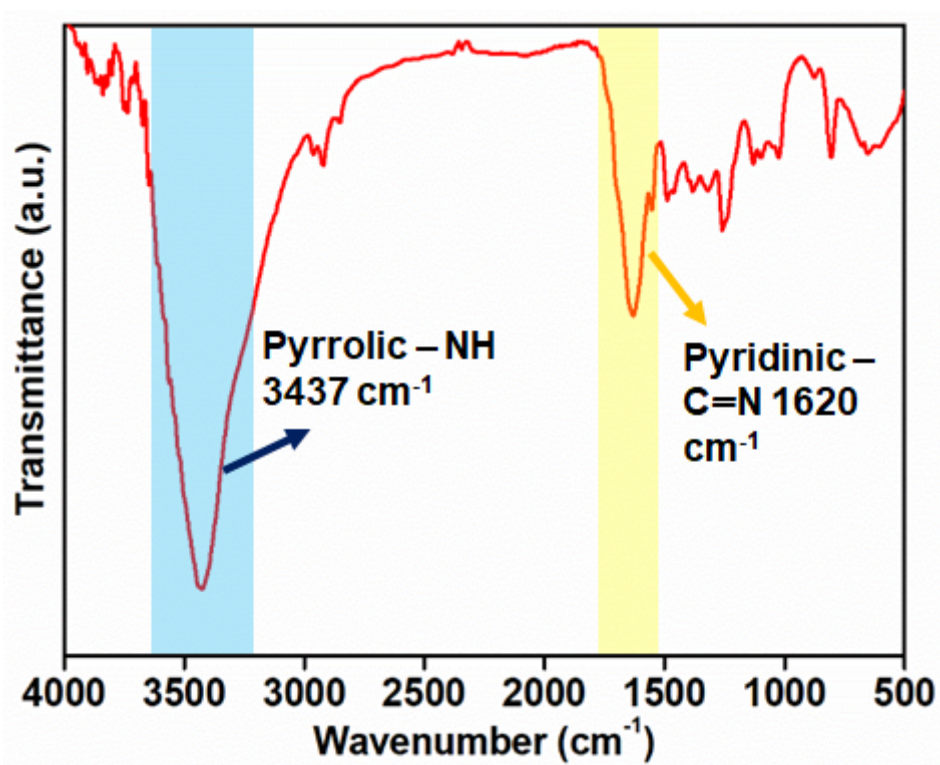


Figure S6: FT-IR spectrum of Ru@Bpy-POP

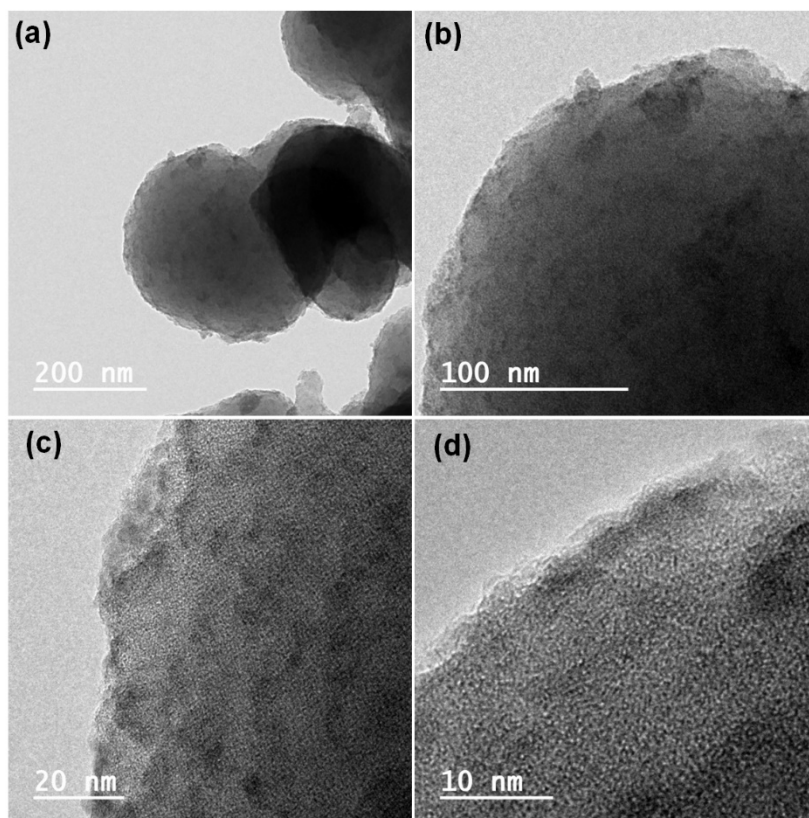


Figure S7: (a & b) TEM images in the low magnification and (c & d) high magnification of Ru@Bpy-POP.

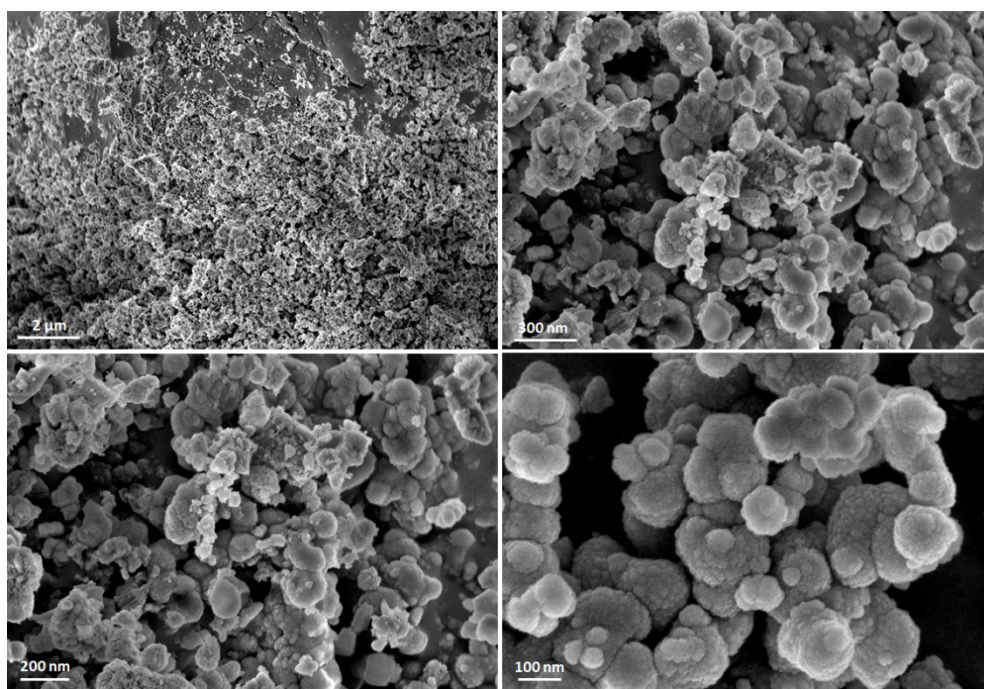


Figure S8: FE-SEM images of Ru@Bpy-POP.

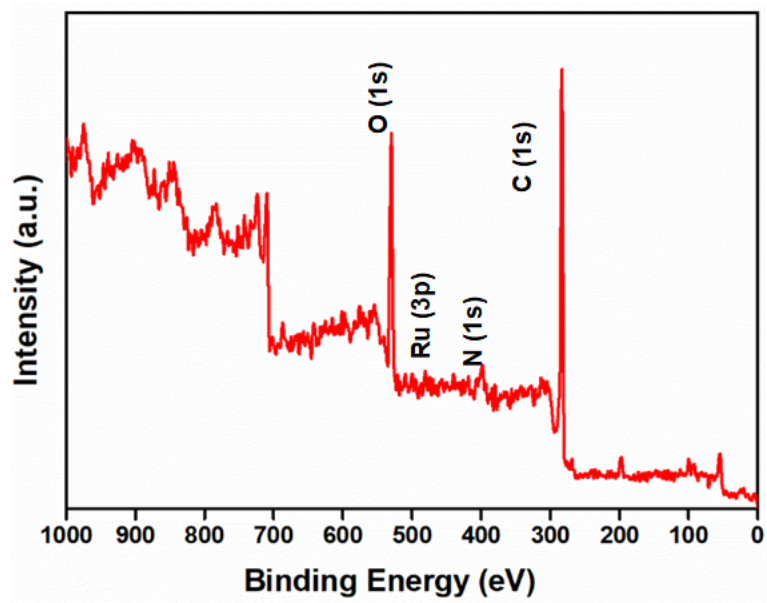


Figure S9: XPS survey spectrum of Ru@Bpy-POP

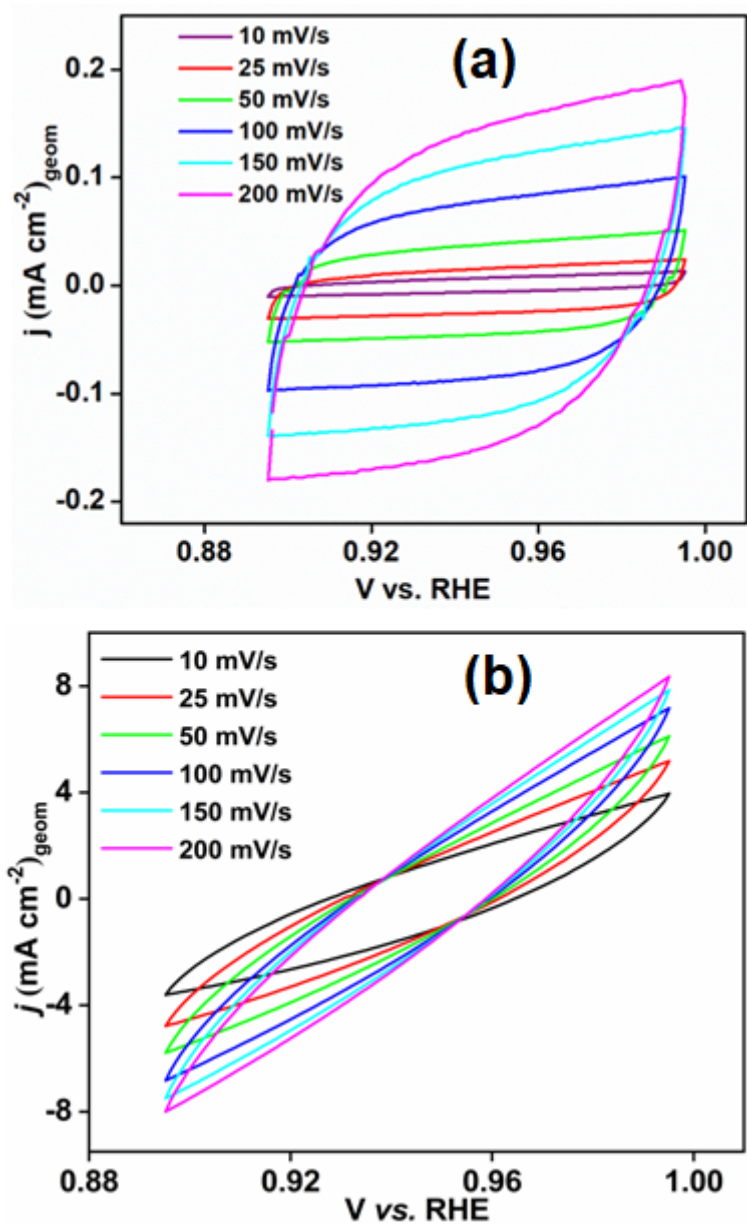


Figure S10: Cyclic voltammetry (CV) of Ru@Bpy-POP (a) & RuO₂ (b) at different scan rates (10, 25, 50, 100, 150, and 200 mV s^{-1}) for ECSA and C_{dl} calculation.

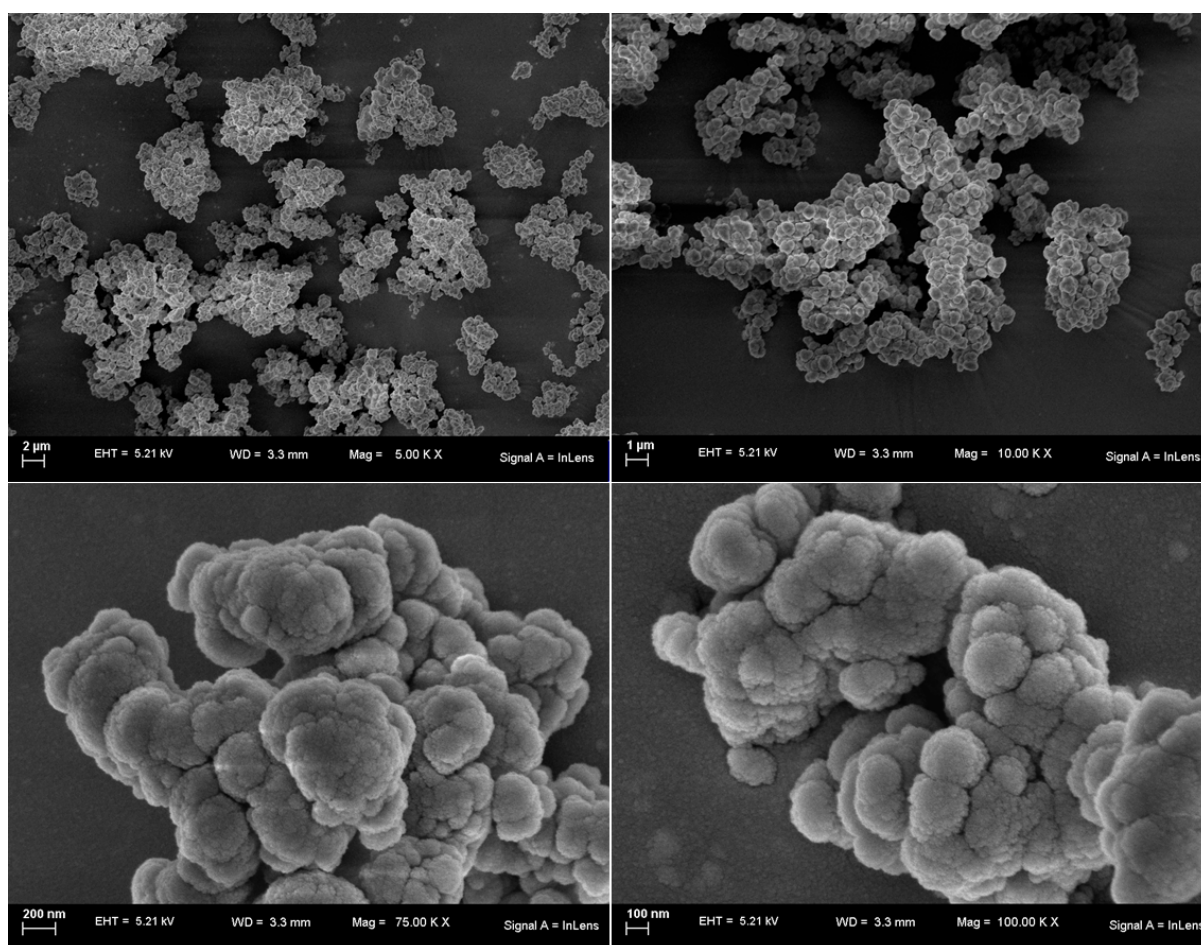


Figure S11: FE-SEM images of Reused catalyst **Ru@Bpy-POP**.

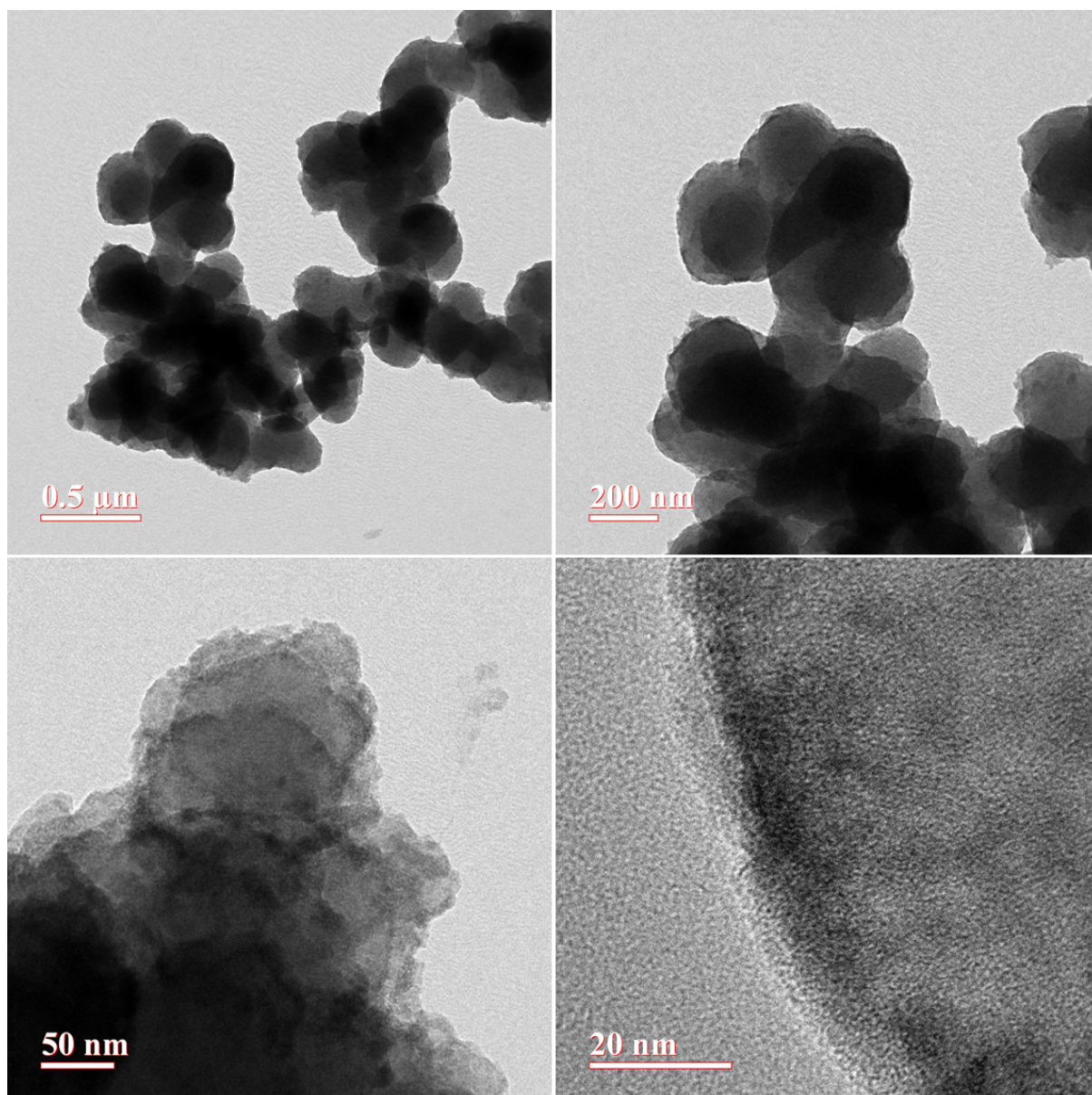


Figure S12: TEM images of Reused catalyst **Ru@Bpy-POP**.

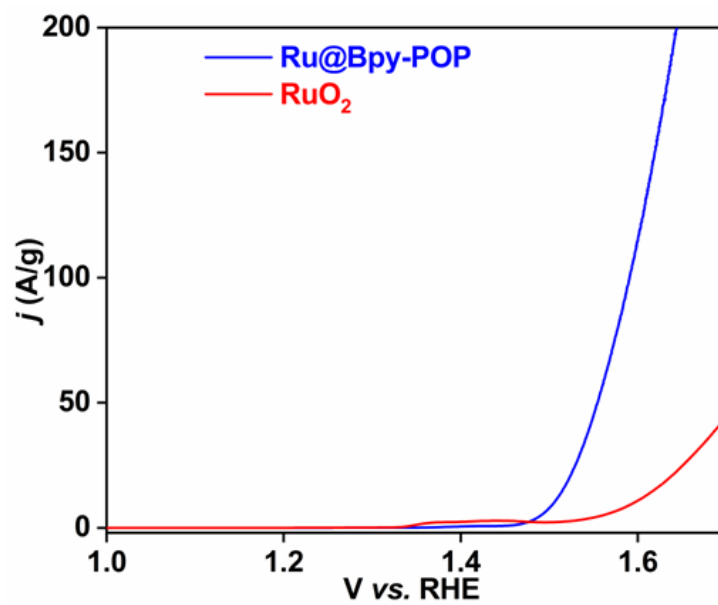


Figure S13: Polarization curve obtained from the mass normalized activity of **Ru@Bpy-POP** (blue) and RuO₂ (red).

References

- (1) C. C. L. McCrory, S. Jung, J. C. Peters and T. F. Jaramillo, *J. Am. Chem. Soc.* 2013, **135**, 16977-16987.